



HAL
open science

Investigations of microbubble-cell interactions during the sonoporation process

Anthony Delalande, Patrick Midoux, Chantal Pichon, Spiros Kotopoulos,
Michiel Postema

► **To cite this version:**

Anthony Delalande, Patrick Midoux, Chantal Pichon, Spiros Kotopoulos, Michiel Postema. Investigations of microbubble-cell interactions during the sonoporation process. 18th International Congress on Sound and Vibration, Rio de Janeiro, Brazil, 10-14 July 2011, Jul 2011, Rio de Janeiro, Brazil. hal-03195597

HAL Id: hal-03195597

<https://hal.science/hal-03195597v1>

Submitted on 11 Apr 2021

HAL is a multi-disciplinary open access archive for the deposit and dissemination of scientific research documents, whether they are published or not. The documents may come from teaching and research institutions in France or abroad, or from public or private research centers.

L'archive ouverte pluridisciplinaire **HAL**, est destinée au dépôt et à la diffusion de documents scientifiques de niveau recherche, publiés ou non, émanant des établissements d'enseignement et de recherche français ou étrangers, des laboratoires publics ou privés.

INVESTIGATIONS OF MICROBUBBLE-CELL INTERACTIONS DURING THE SONOPORATION PROCESS

Anthony Delalande, Patrick Midoux, **Chantal Pichon**

Centre de Biophysique Moléculaire UPR 4301 CNRS, rue Charles Sadron 45071 Orléans Cedex 2, France

e-mail: chantal.pichon@cnrs-orleans.fr

Spiros Kotopoulis

Department of Engineering, The University of Hull, Cottingham Road, Kingston upon Hull HU6 7RX, United Kingdom

Michiel Postema

Department of Physics and Technology, University of Bergen, Allégaten 55, 5007 Bergen, Norway

Ultrasound (US) stimulation coupled to gaseous microbubbles (MB) is a new technique for efficient drug/gene delivery. Upon US exposure, MBs can be expanded, moved and even destroyed. These properties offer the opportunity of site-specific local drug delivery.

A key to success of this technique lies in understanding mechanisms governing microbubble-cells interactions. Several studies suggest that pore formation is less likely to be the dominant mechanism. However, recent data have suggested that endocytosis mechanisms might also be involved. Real time experiments of sonoporation were performed to investigate how MB behaves towards cells, under optimal conditions that allow an efficient gene transfer. Studies have been done with a specific experimental set-up combining a CCD of a PHOTRON FastCam MC-2.1 high-speed camera connected to LSM 500 META Zeiss fluorescence confocal microscope. The transducer was placed in a custom-built sonoporation chamber mounted on the confocal microscopy. Bubbles and plasmid encoding the gene of interest (pDNA) were fluorescent-labelled. Our data showed that small size bubbles were pushed and entered the cell during the sonoporation processes. Optical sections of the cell support this entry. The intracellular fate of MB and pDNA following sonoporation was investigated by confocal microscopy investigations on cells that express different fluorescent markers of cellular compartments. We observed that molecule with large size as pDNA (3 MDa) was mainly localized close at plasma membrane straightaway following insonation. At later time, punctuate staining like vesicles were progressively moved towards the nucleus. They were localized in late endosomes 3h post insonation and very few reached the nucleus after 6h. We are currently investigating if there is a specific plasma membrane area that is prone to be destabilized by sonoporation. Data emerging from these different studies will allow specifying limitations of US assisted MB delivery and to fine tune MB composition for gene delivery.

1. Introduction

Activation of microbubbles (MB) under specific ultrasound (US) beams induces a transient cell membrane permeabilization with a process known as sonoporation [1-3]. Sonoporation is the transient permeabilization and resealing of a cell membrane with help of ultrasound and/or an ultrasound contrast agent, allowing for the trans-membrane delivery and cellular uptake of macromolecules up to 3 MDa. Many studies have demonstrated increased drug and gene delivery of sites under US application, presumably owing to sonoporation. In the field of gene transfer, several studies have reported an improvement of gene delivery by US assisted MB [4].

Although mechanical disruption with the aid of ultrasound has been attributed to violent side effects of inertial cavitation and microbubble fragmentation, most notably, the increased uptake has also been observed at low acoustic amplitudes, *i.e.*, in acoustic regimes where inertial cavitation and microbubble fragmentation are not to be expected. An US contrast agent microbubble might act as a vehicle to carry a drug or gene load to a perfused region of interest. If the same ultrasound field that has been implicated in the sonoporation process can cause release of the therapeutic load, this load could be delivered into cells. Apart from plainly mixing ultrasound contrast agents with therapeutic agents, several schemes have been proposed to incorporate therapeutic loads to microbubbles.

Several studies have been conducted these last years to delineate mechanisms involved in US mediated delivery [5-8]. However, it is still unclear exactly how cells that are subjected to US and MB internalize extracellular compounds, and which cellular responses US and MB evoke.

As others, we have shown that sonoporation can also induce an outward transport of small intracellular molecules that likely due to membrane destabilization [8]. The permeabilization engenders a transient release of small molecules such as enhanced green fluorescent protein (eGFP) from the cytosol of HeLa cells stably expressing eGFP gene while preserving cell viability. Results obtained in that study, using BR14 Bracco's MB, reinforced the hypothesis of transient pore formation mechanism induced by sonoporation. However, this seems not to be the unique mechanism that is involved in sonoporation. Indeed, the contribution of endocytosis besides pore formation for the uptake of extracellular molecules by sonoporation has been proposed recently [9]. If so, an improved knowledge on both the extracellular and intracellular fates of MB and the cargo need to be acquired to clearly specify limitations and to further improve the system.

The study aimed at acquiring knowledge on microbubble-cell interactions during sonoporation by following the intracellular fate of microbubbles and plasmid DNA (pDNA) as cargo inside cancer cells. Investigations were performed on HeLa cells, human cervix cancer cells that stably express protein markers of intracellular organelles which are fused with enhanced green fluorescent protein (eGFP) as fluorescent tag. We have established these cells to delineate intracellular routing of pDNA delivered by our chemical vectors [10] and Billiet et al., 2011 under submission). Data shown were obtained with HeLa cells expressing either the small GTPase Rab7-eGFP or the nucleoporin Nup153-eGFP. Rab7 and Nup153 are commonly used as marker of late endosomes and nuclear pore, respectively. Therefore, these fluorescent chimera molecules are useful to delimit easily the late endosomal compartments and the nucleus in live cells. Sonoporation was performed with MicromarkerTM bubbles. The pDNA and MB were labelled with fluorescent tags to follow their localization inside cells upon sonoporation.

2. Material and Methods

2.1 Cell culture

HeLa cells (ATCC CCL-2) were immortalized cells derived from the cervix adenocarcinoma of a young American female. HeLa-Rab7-eGFP and HeLa Nup153-eGFP cells are HeLa cells that were stably transfected with plasmid encoding Rab7 and Nup153 genes fused with eGFP gene, respectively. The stable clones used in this study were obtained upon cell sorting by flow cytometry. Cells were cultured in MEM with Earl's salts medium supplemented with 10% v/v heat-inactivated fetal

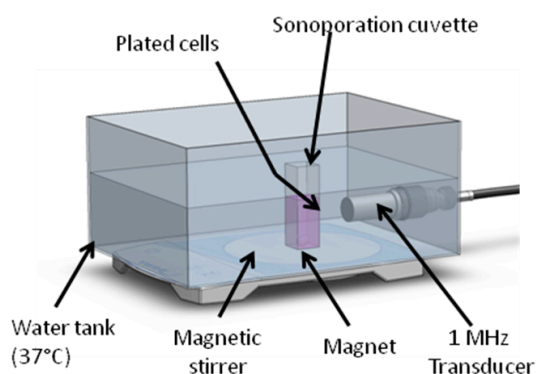
calf serum (FCS), GlutaMAXTM (LifeTechnologies Gibco, Paisley, Renfrewshire, UK), 1% v/v of non-essential amino-acids, penicillin (100 units/ml) and streptomycin (100 µg/ml), at 37°C in a humidified atmosphere containing 5% CO₂.

2.2 Plasmids

The reporter plasmid DNA used was a homemade plasmid of 7.5 kb that encodes the firefly luciferase gene under control of the strong cytomegalovirus (CMV) promoter. Five consecutive κB motifs that recognize the NFκB transcription factor have been inserted upstream of the promoter [11]. pDNA was labelled with cyanin 3 (Cy3) using the Label IT nucleic acid labelling kit (Mirus, Madison, WI, USA) at 1 : 2 reagent/pDNA weight ratio according to the manufacturer's instructions. The labelled DNA was purified by ethanol precipitation. The labeling density determined by absorbance according to the manufacturer's protocol was 1Cy3 per 80 bp.

2.3 Microbubbles and ultrasound set-up

MicroMarkerTM MBs were provided from VisualSonics B.V. (Amsterdam, Netherlands). They are composed of perfluorobutan gas encapsulated in a phospholipid shell. MicromarkerTM (MM) microbubbles have a mean diameter of 2.3-2.9 µm. MM were prepared a few minutes before experimentation according to the manufacturer's protocol. The experimental set-up used is shown below.



US waves were generated from a 0.5 inches transducer with 1 MHz frequency (IBMF-014, Sofranel, Sartrouville, France). The transducer was driven with an electrical signal generated by an arbitrary waveform generator (Agilent 33220A, Agilent technologies) and amplified with a power amplifier (ADECE, Artannes, France). Pulsed ultrasound (10 kHz) with a duty cycle of 40% was used in this study. The negative peak acoustic pressures investigated were measured in a separate set-up with a calibrated HLG-200 capsule

hydrophone (Onda, Dahm International ApS, Denmark) at 3 cm depth, the natural focal distance of the transducer. The hydrophone was positioned inside the insonation cuvette. The attenuation of the cuvette walls was measured separately and found to be negligible at the frequency 1 MHz (less than 10%). We therefore did not expect significant standing waves to be generated inside the cuvette. 10⁵ cells were seeded on a center portion of Opticell[®] membrane (1 x 1.5 cm) one day prior sonoporation experiments. After washing with Opti-MEM (Invitrogen, Carlsbad, CA) supplemented with 1% FCS, the Opticell[®] was placed inside the cuvette and the sonoporation was performed as indicated.

2.4 Luciferase assay

The transfection efficiency of pDNA encoding luciferase gene was determined by measuring the luciferase activity in cell lysate. The Relative Light Units (RLU) was measured with a Lumat LB9507 luminometer (Berthold, Wildbarch-Germany) after adding 100 µl of luciferase substrate (1mM luciferin containing ATP) to 60 µl of cell lysates and expressed as RLU per mg of proteins. Proteins content of cell lysates were quantified by bicinchoninic acid assay [12].

2.5 High speed camera and confocal fluorescence microscopy

An overview of the setup used for the fluorescence experiments is shown in Figure 4. A custom-made aluminium sonication chamber with internal dimensions of 130 × 170 × 35 mm³ was locked into to the xy-stage of a 200M inverted confocal microscope (Carl Zeiss AG, Oberkochen, Germa-

ny) coupled with a LSM Axiovert 510 scanning device (Carl Zeiss), using an EC Plan-Neofluar 40×/1.30 oil DIC M27 objective (Carl Zeiss AG), with automated z-stack functionality.

The peak-negative acoustic pressure was measured at the objective's field of view and corresponded to $MI=0.2$. An OptiCell[®] cell culture chamber (Nunc GmbH & Co. KG, Langenselbold, Germany) was placed on the sonication chamber. On one side of the cell culture chamber was seeded a monolayer HeLa cells (1×10^6). Prior to injection in the OptiCell[®], MicroMarker contrast agent was labelled using a DiD (DiI_{C18}(5), $\lambda_{exc}=633$ nm and $\lambda_{em}=649-703$ nm) lipophilic fluorescent probe (Vybrant[™], Molecular probes, Invitrogen, San Diego, CA, USA). A ratio of 1 μ l of DiD to 40 μ l MicroMarker was homogenized by pipetting and incubating for 5 minutes at room temperature. MBs were injected into the cell culturing chamber before each experiment. The signal consisted of 40 cycles with a centre frequency of 1 MHz and a pulse repetition frequency of 10 kHz, with a maximum MI of 0.15.

3. Results and discussion

The optimal acoustic parameters that give the maximal gene transfer have been first determined on adherent HeLa cells. Our data indicate that the luciferase gene expression was dependent on the acoustic parameters and the presence of MB. We found that optimal parameters that gave a maximum luciferase gene expression without significant toxicity at 1 MHz of US was 150kPa, 40% duty cycle, 60 sec of exposure time in presence of 10^7 bubbles. As an example, shown in Figure 1 are the levels of luciferase expression as function of acoustic pressure.

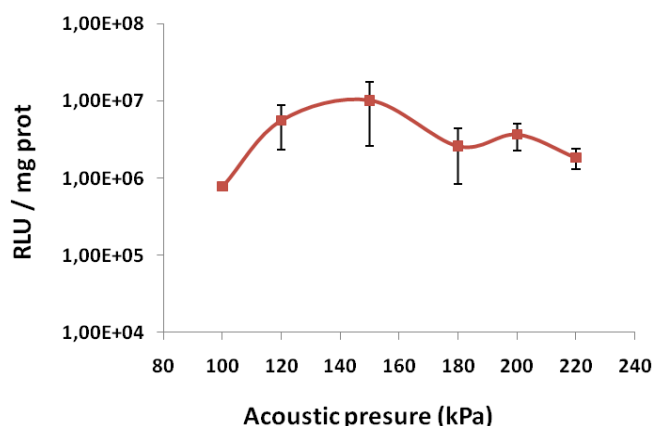


Figure 1: Influence of acoustic pressure on gene transfer efficiency.

Cells were sonoporated at US of 1MHz, 40% duty cycle and 60 sec of exposure time in presence of 5 μ g of pDNA and 10^7 bubbles. Then, they were further incubated at 37°C during 24h before determining the luciferase activity which is expressed as RLU/mg of proteins. Values shown are means of 2 experiments done in duplicate.

A key to success of this technique lies in understanding mechanism governing MB and cell interactions. Real time confocal microscopy investigations were performed on adherent cells using pDNA and MB labeled with Cy3 (red) and DiD (blue) lipophilic tracer, respectively. The first experiments were done on HeLa cells with pDNA-tagged Cy3 which was mainly localized as red spots at plasma membrane straightaway following sonoporation. At later time, these spots progressively moved inside cells (not shown). The structures could correspond either to vesicles (endosome) or aggregates like structures upon sonoporation. To distinguish between these 2 possibilities, kinetic experiments were performed in HeLa cells to investigate if pDNA and MB reached some endocytic organelles upon sonoporation. Data presented in figure 2 were obtained with HeLa cells expressing Rab7-eGFP (green) which are localized on the surface of late endosomes, intracellular compartments in which end up internalized molecules before being delivered into lysosomes for degradation. Upon sonoporation, pDNA were localized mainly at the plasma membrane and without colocalization with Rab7-eGFP (figure 2A and 2B).

Observations made 3 h post-sonoporation before indicated that some of pDNA but not all ended up into late endosomes as demonstrated by yellow staining (merge of green and red spots) indicating

their localization in Rab7 positive organelles (figure 2C and D). The presence of punctuate red staining corresponding to pDNA could correspond to pDNA that are either free (present inside the cytosol upon sonoporation) or routed in another intracellular compartments different to late endosomes.

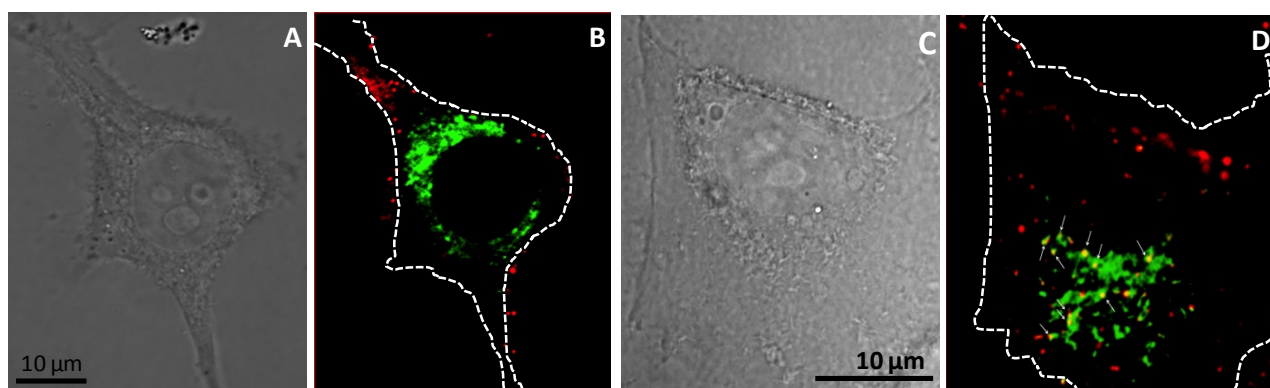


Figure 2: Localization of pDNA relative to late endosomes.

HeLa Rab7-eGFP cells were sonoporated at optimal acoustic parameters in presence of 2.5 µg of Cy3-tagged pDNA and MB. Green and red staining correspond to Rab7-eGFP positive late endosomes and pDNA-Cy3, respectively. Yellow color corresponds to a co-localization of pDNA and Rab7 (arrows). Confocal microscopy observations were made either immediately after sonoporation (A, B) or 3 hours post-sonoporation (C, D). A and C: phase contrast images; B and D: merge of green and red fluorescence images. White dotted lines in the right frames indicate the cell plasma membrane boundary.

MB labelled with DiD were used to follow their fate in HeLa cells expressing Nup153-eGFP that delimit the cell nucleus. The representative analysis shown in Figure 3 was acquired 6h post-sonoporation. Strikingly, we found that in addition to pDNA (red) which are observed throughout the cytoplasm as in Figure 2, blue spots that likely correspond to MB-tagged DiD were also observed inside cells. Our observations indicated also that pDNA were not efficiently delivered into the nucleus. However, it is worth noticing that some spots were close to the nucleus as indicated by their localization in the vicinity of nuclear envelope delimited by Nup153-eGFP.

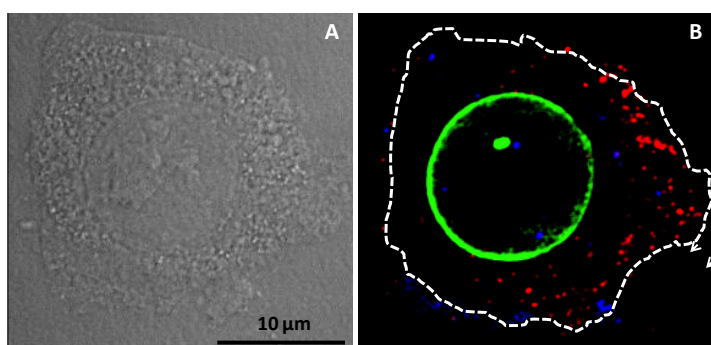


Figure 3: Localization of pDNA relative to the nucleus 6h post-sonoporation.

HeLa Nup153-eGFP cells were sonoporated at optimal acoustic parameters in presence of 2.5 µg of Cy3-tagged pDNA (red) and DiD labelled MB (blue). The green staining corresponds to Nup153-eGFP which delimits the cell nucleus. White dotted lines in the right frames indicate the cell plasma membrane boundary.

The presence of MB inside cells raises the question of their intracellular entry pathway. Do they enter inside cells during the sonoporation process or as a consequence of the sonoporation following their interaction with cells? The behavior of liposomes based-MB under ultrasonic waves has been studied by predictive models and high speed optical imaging methods [13, 14]. Data obtained from studies performed at low acoustic amplitudes have shown that lipid-shelled MB can undergo destruction with microjetting, fragmentation or coalescence under US waves. These responses are dependent on the size, the physico-chemical features of the lipid shell. We performed real time experiments of sonoporation event to investigate how MB behaves towards cells, under our conditions. For that, we developed an experimental set-up combining a color charge coupled device of a

PHOTRON FastCam MC-2.1 high-speed camera connected to LSM 500 META Zeiss fluorescence confocal microscope (Figure 4). The transducer was placed in a custom-built sonication chamber, in which an OptiCell[®] was mounted. We found that at low mechanical index (< 0.15) at 1 MHz, MB clusters can be formed and pushed within seconds towards cell plasma membrane (not shown). This is in agreement with our recent *in vitro* data showing that microclusters consisting of lipid-encapsulated microbubbles can be formed using primary and secondary radiation forces, and pushed towards vessel walls [15]. Interestingly, we also recorded events showing oscillating MB with a small size entered inside cells in few seconds (~ 10 s) and others that remained stuck on the plasma membrane (Figure 4).

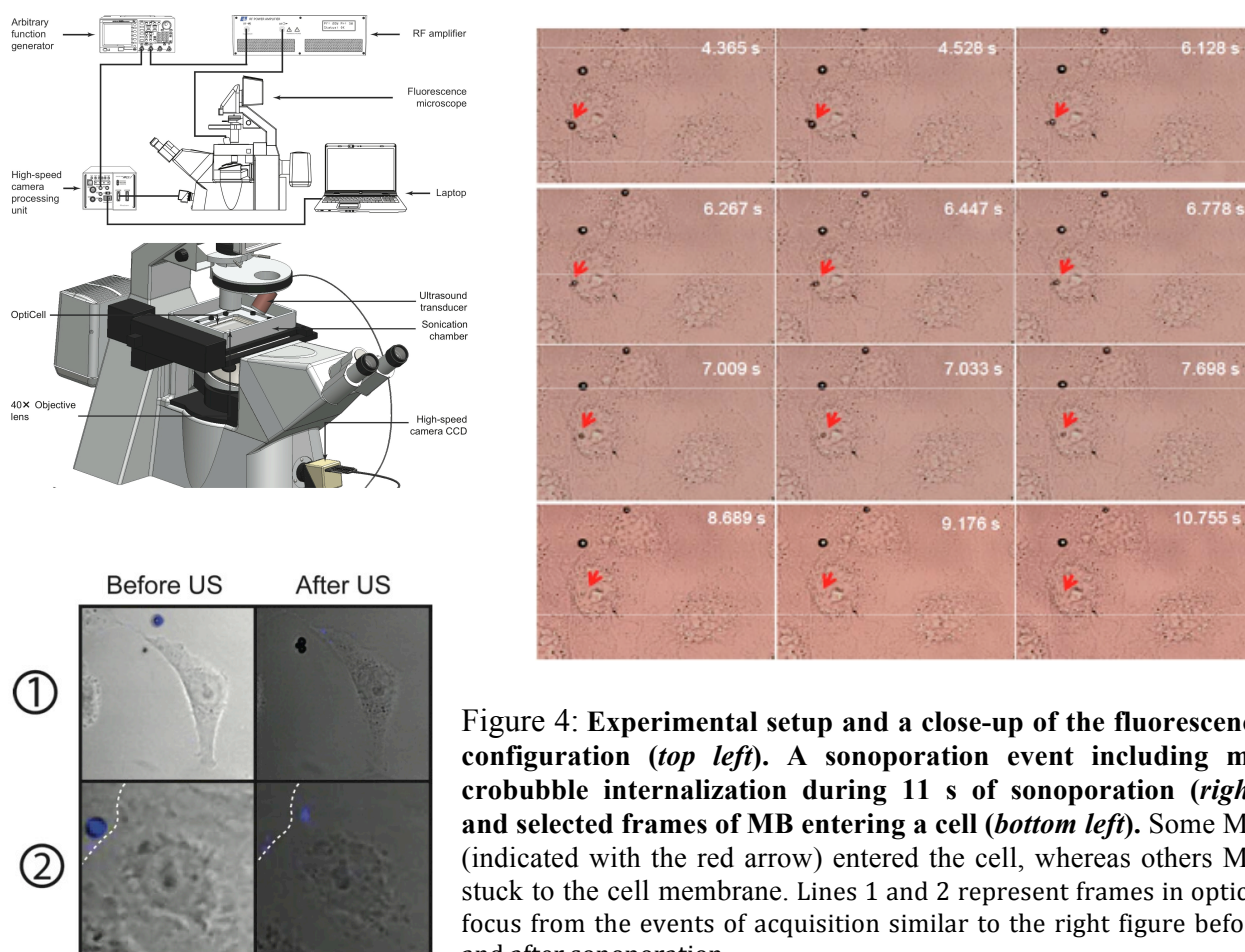


Figure 4: Experimental setup and a close-up of the fluorescence configuration (*top left*). A sonoporation event including microbubble internalization during 11 s of sonoporation (*right*) and selected frames of MB entering a cell (*bottom left*). Some MB (indicated with the red arrow) entered the cell, whereas others MB stuck to the cell membrane. Lines 1 and 2 represent frames in optical focus from the events of acquisition similar to the right figure before and after sonoporation.

Our set up analysis was checked to rule out that the motion of MB takes place in a plane different from that of the cell. This was also validated by fluorescence confocal microscopy analysis. When MB labeled with DiD lipophilic tracer were used, our observations indicated that MB were inside the cell just below the plasma membrane (Figure 4 columns a and b).

In summary, data obtained from this study confirmed that pDNA that enters inside cells during sonoporation reaches endocytosis pathway as confirmed by its localization inside late endosomes which are Rab7 positive organelles. A set-up combining high speed camera coupled with confocal fluorescence microscopy has allowed us to observe that some MB were forced to enter the cell during sonoporation whilst other were stuck at the plasma. Altogether our results point out acoustically active microbubbles incorporating the drug inside could release it inside cells.

4. References

1. Bao, S., B.D. Thrall, and D.L. Miller, *Transfection of a reporter plasmid into cultured cells by sonoporation in vitro*. *Ultrasound Med Biol*, 1997. **23**(6): p. 953-9.
2. Miller, D.L., S. Bao, and J.E. Morris, *Sonoporation of cultured cells in the rotating tube exposure system*. *Ultrasound Med Biol*, 1999. **25**(1): p. 143-9.
3. Taniyama, Y., et al., *Local delivery of plasmid DNA into rat carotid artery using ultrasound*. *Circulation*, 2002. **105**(10): p. 1233-9.
4. Wang, X., et al., *Gene transfer with microbubble ultrasound and plasmid DNA into skeletal muscle of mice: comparison between commercially available microbubble contrast agents*. *Radiology*, 2005. **237**(1): p. 224-9.
5. van Wamel, A., et al., *Vibrating microbubbles poking individual cells: drug transfer into cells via sonoporation*. *J Control Release*, 2006. **112**(2): p. 149-55.
6. Duvshani-Eshet, M., et al., *Therapeutic ultrasound-mediated DNA to cell and nucleus: bio-effects revealed by confocal and atomic force microscopy*. *Gene Ther*, 2006. **13**(2): p. 163-72.
7. Duvshani-Eshet, M., D. Adam, and M. Machluf, *The effects of albumin-coated microbubbles in DNA delivery mediated by therapeutic ultrasound*. *J Control Release*, 2006. **112**(2): p. 156-66.
8. Kaddur, K., et al., *Transient transmembrane release of green fluorescent proteins with sonoporation*. *IEEE Trans Ultrason Ferroelectr Freq Control*, 2010. **57**(7): p. 1558-67.
9. Meijering, B.D., et al., *Ultrasound and microbubble-targeted delivery of macromolecules is regulated by induction of endocytosis and pore formation*. *Circ Res*, 2009. **104**(5): p. 679-87.
10. Pichon, C., L. Billiet, and P. Midoux, *Chemical vectors for gene delivery: uptake and intracellular trafficking*. *Curr Opin Biotechnol*, 2010. **21**(5): p. 640-5.
11. Goncalves, C., et al., *An optimized extended DNA kappa B site that enhances plasmid DNA nuclear import and gene expression*. *J Gene Med*, 2009. **11**(5): p. 401-11.
12. Smith, P.K., et al., *Measurement of protein using bicinchoninic acid*. *Anal Biochem*, 1985. **150**(1): p. 76-85.
13. Doinikov, A.A., J.F. Haac, and P.A. Dayton, *Modeling of nonlinear viscous stress in encapsulating shells of lipid-coated contrast agent microbubbles*. *Ultrasonics*, 2009. **49**(2): p. 269-75.
14. Postema, M. and G. Schmitz, *Ultrasonic bubbles in medicine: influence of the shell*. *Ultrason Sonochem*, 2007. **14**(4): p. 438-44.
15. Kotopoulis, S. and M. Postema, *Microfoam formation in a capillary*. *Ultrasonics*. **50**(2): p. 260-8.